Journal of Metals, Materials and Minerals, 35(1), e1917, 2025

Durability of precast prestressed concrete pile in exposure severe environment

Nantawat KHOMWAN[1,*], and Pinai MUNGSANTISUK[2]

[1] *Department of Civil Engineering, Faculty of Engineering at Kamphaeng Saen, Kasetsart University, Nakhon Pathom 73140, Thailand*
[2] *Thai Marine Protection, 555/8 Moo12, Tambon Bangphasi, Amphoe Bang Len, Nakhon Pathom, 73130, Thailand*

***Corresponding author e-mail**: fengnwk@ku.ac.th

Received date:
15 December 2023
Revised date:
8 May 2024
Accepted date:
24 December 2024

Keywords:
Durability;
Precast prestressed concrete pile;
Exposure severe environment

Abstract

This research project focuses on studying the corrosion resistance of precast prestressed concrete (PC) piles under severe conditions. All PC and non-PC samples were cast using Portland cement type III. The samples included 1 m and 6 m length specimens. To evaluate the effectiveness of corrosion prevention, Sacrificial Anode Cathodic Protection (SACP) was installed in the specimens. Various durability properties of concrete were tested, including chloride permeability, concrete resistivity, and half-cell potential. For short-term effects, an electrical accelerated condition was conducted for the 1 m specimens, which were submerged in a 5% sodium chloride solution by weight. Experimental studies were carried out to evaluate the 100 mV polarization shift criterion for confirming the effectiveness of SACP in arresting the progress of corrosion in steel. In addition, for long-term effects and under more realistic conditions, 6 m full-scale PC specimens were installed in a high salinity area to evaluate durability and corrosion behavior. Four different types of sacrificial anodes were used to evaluate durability and corrosion behavior, and corrosion current assessments were closely monitored. The findings from these studies provide vital parameters for the repair and maintenance process, with the aim of minimizing structural loss. The results of this study are intended to guide the decision-making process for developing effective repair strategies.

1. Introduction

The deterioration of prestressed concrete structures due to the chemical attack-induced corrosion of prestressed steel wire or steel reinforcement is of concern [1]. Especially for corroded prestressed wire, it may cause sudden failure, causing the loss of life. The corrosion rate of the steel not only affects the speed at which corrosion products form and accumulate, influencing the performance and serviceability of PC structures, but also impacts the force of prestressing members and the rate at which the effective cross-sectional area of steel reinforcement is reduced. Corrosion initiation and propagation of steel reinforcement reduces the service life of structures induced by the cracking/spalling of concrete cover or effective steel cross-section area/strength degradation. Because of the severe environment, the impact of soil or marine corrosion on critical infrastructure in actual condition is significant. NACE Impact Report states that half of the structures require major repair within ten years after construction [2]. To avoid catastrophic building failures, it's crucial to consider the impact of corrosion rates on safety assessments, maintenance planning, and predicting the remaining lifespan of current structures.

In order to prolong the lifespan of structures, cathodic protection (CP) is an electrochemical method utilized to reduce the corrosion rate in reinforced concrete structures without removing chloride from contaminated concrete [3-8]. The fundamental principle of CP is to supply a suitable cathodic polarization current to the protected structure, thereby shifting its potential in a negative direction to either reduce the corrosion rate or induce passivation in the steel [9,10]. Thus, SACP uses zinc covered with encapsulating mortar with lower electrochemical potentials than steels or cathodes. The encapsulating mortar has become a key parameter for potential difference [11]. The difference in potential between the anodes and cathodes is used to protect the structure. SACP has more advantages than conventional repair techniques, such as patchwork, because it is used directly to stop corrosion activity and requires less maintenance and monitoring, especially to overcome the risk of hydrogen embrittlement in prestressed steel. In addition, sacrificial anode installation has recently become a common practice in the UK [12]. However, only a few structures are installed CP systems to RC systems reported by [13]. Because of these limitations, such as evidence of long-term use, knowledge of corrosion and CP system and national standards/ guidelines are the main barriers [14]. However, there is insufficient information in the published literature about the salt attacks on long-term exposure of the buildings, especially in precast prestressed concrete piles, a commonly-used form of building foundation that supports structures.

The objective of the paper is organized in the following manner: first, 1meter prestressed and non-prestressed specimens were conducted. The specimens were installed in different types of sacrificial anodes. All specimens were electrically accelerated and immersed in 5% sodium chloride by weight. Four types of sacrificial anodes performance and the factors affecting the short-term behavior were tested and reported, including chloride permeability, concrete resistivity, half-cell potential and 100 mV decay shift criteria. After that, for the second part, an experimental program was focused on evaluating the 6 m

full-scale prestressed samples constructed in severe actual conditions. The long-term performance of the SACP system was demonstrated.

2. Experimental

2.1 Materials and mix proportion

The specimen preparation involved the use of Type III Portland cement, which met the requirements of ASTM C150. Coarse aggregate comprised crushed limestone with a maximum size of 20 mm, while fine aggregate consisted of natural sand. The specific gravity was 2.70 for coarse aggregate and 2.60 for fine aggregate. To achieve the desired workable conditions, high-range water-reducing admixtures with a specific gravity of 1.18 were added. The water-to-cement ratio (w/cm) was maintained at 0.38. The concrete exhibited a compressive strength of 35 MPa at 28 days and a slump of 8 cm. For further details, please refer to Table 1, which outlines the mix proportions of the specimens.

2.2 Mixing, specimen preparation and curing

The concrete mixing occurred at a concrete plant using a horizontal mixer, and the process followed the manufacturer's guidelines. To initiate the mixing, the mixer was thoroughly cleaned and washed. Cement was then loaded into the mixer, followed by the aggregates and water with dissolved admixture. All the materials were thoroughly mixed to produce concrete. The specimens were left in the mold for 24 h under a moist cover before demolding. Subsequently, all specimens were sprayed with water twice a day, and the concrete remained damp for seven days before being lifted, transported, and submerged in a sodium chloride solution.

Three sets of specimens were cast: PC (1 m pile), non-PC cylinder, and large PC specimen (6 m pile). For the first set, all ten specimens had identical 180 mm square cross-sections and 1000 mm in length. Before casting, they were all prestressed with four main reinforcing 4 mm diameter steel wires. Secondly, six-cylinder specimens of 150 mm diameter with 300 mm height were prepared for non-PC cylinders. Each specimen was centrally embedded with a non-prestressed 4 mm steel wire. This experimental study was carried out to study the corrosion effect of non-prestressed steel wire. In addition, four prestressed specimens were cast in this study to evaluate the effectiveness of the sacrificial anode in actual conditions. The specimens were 180 mm cross-section and 6 m in length. The steel wires were installed and prestressed before concrete pouring. The specimen schematic representation is shown in Figure 1, and the preparation procedure is represented in Figure 2.

The steel wire reinforcement was electrically connected for sacrificial anode installation. Sacrificial anodes, known for their effectiveness, were installed on the PC wire. A multi-meter was used to verify the anode connection and its effectiveness, providing a reassuring measure of the process. Electrical continuity was measured between the anode tie wires and reinforcing steel, with the suggested electrical connection resistance being less than 1 ohm for proper installation according to ISO standard [15]. Four types of sacrificial anodes, namely CB20, CR20, CR40, and CR60, were installed, as shown in Figure 3. "B" and "R" stand for bar and round shape. The nominal amount of zinc weight was 20 g, 40 g, and 60 g. The CR60, in particular, demonstrated a robust corrosion prevention performance for steel reinforcing bars in the earlier study reported in [11]. There were two specimens in each group. The control (CT) specimens and the sacrificial anode specimens are CB20, CR20, CR40 and CR60. The sacrificial anode locations were identical in all specimens of 350 mm from one end. For non-prestressed cylinder specimens, there were two control specimens and two sacrificial anode specimens of CB20 and CR60. To investigate in actual condition, each large PC specimen (6 m pile) was pre-installed with different sacrificial anode types of the anode spacing at 750 mm, 1200 mm, and 1500 mm for CB20/CR20, CR40, and CR60, respectively. Finally, after concrete curing, the large PC specimens were driven to the construction site.

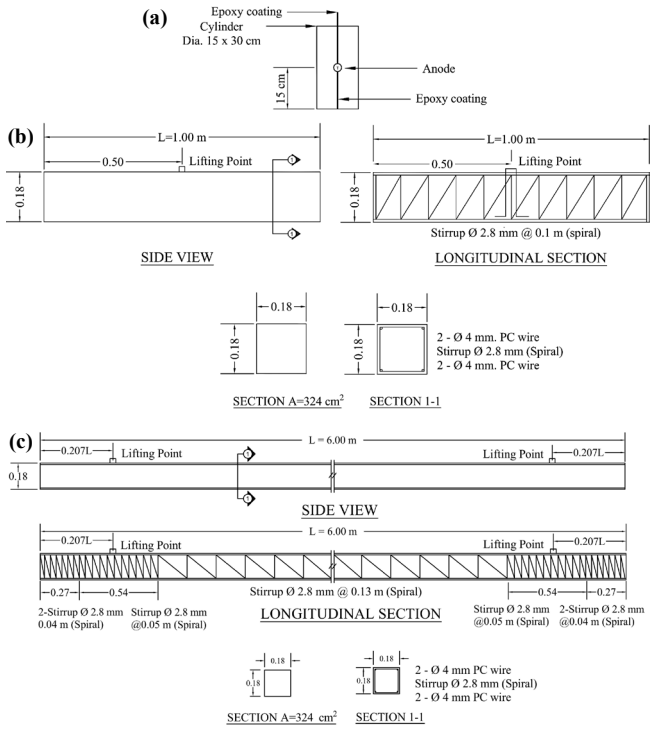

Figure 1. Specimen dimension and reinforcement detail; (a) non-PC cylinder, (b) PC, and (c) large PC specimen.

Figure 2. Specimen preparation.

Table 1. Mix proportion (kg·m^{-3}).

Cement	Gravel	Sand	Admixture	Water
400	1157	683	4	152

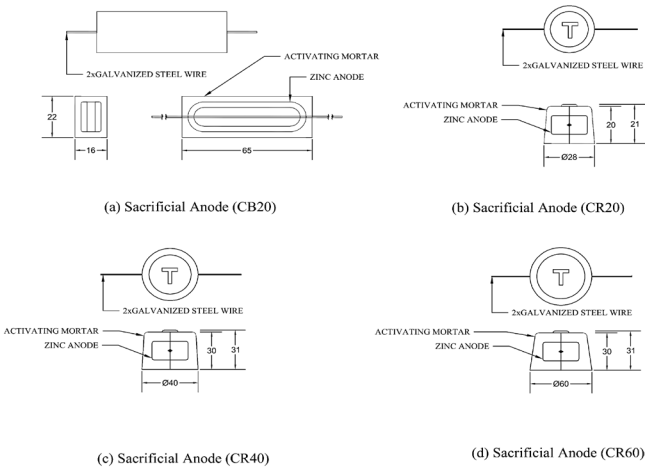

Figure 3. Sacrificial anode type; (a) CB20, (b) CR20, (c) CR40, and (d) CR60.

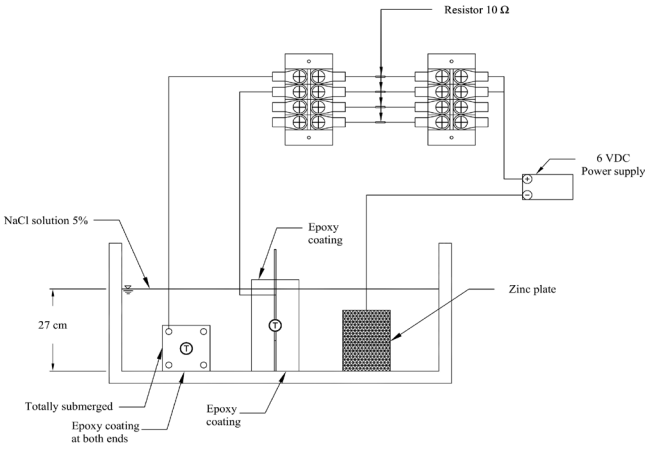

Figure 4. Electrical accelerated test set up.

2.3 Accelerated corrosion method

The electrical accelerated test was conducted for PC specimens and non-PC cylinders at the age of 7 days using a power supply of 6VDC. The specimens were immersed in a 5% sodium chloride solution (by weight). The test schematic setup is shown in Figure 4. The output current from the power supply was recorded every 6 h. The epoxy coating was applied on both ends of the concrete surface, and embedded steel wire was extended out from the concrete to prevent premature corrosion. The test procedures were conducted following the modified NT BUILD 356 [16], and the current is calculated based on Ohm's law by measuring in volts drop across the resistor, as shown in Figure 4. The current was measured every 6 h until specimen failure, when the crack could be detected to 100 mm in length.

The corrosion activity was investigated using half-cell potential method referring to a standard copper/copper-sulfate (CSE) conform to ASTM C876-22b [17]. The half-cell was tested on concrete surface while saturated surface-dried condition. The shift of the 100 mV cathodic polarization criterion described in the EN ISO standard was also evaluated. The time of the first crack was observed, and data was recorded during the accelerated corrosion test. After the failure of each specimen, the specimen was broken, and the PC wire was removed. The weight loss was determined by immersing steel in acid, following designation C.3.5 of ASTM G1 [18] for 10 min to remove rust.

2.4 Long-term exposure of PC pile in actual severe environment

The four large PC specimens were driven in the salinity area at the concrete age of 14 days. The method is to initially jet the pile to a few feet short of the required penetration, then complete the installation by driving with a drop hammer, as shown in Figure 5. The pile elevations and the anode locations of each pile are presented in Figure 6. These piles were considered to evaluate the corrosion effect in actual conditions. As mentioned earlier, the piles were installed using sacrificial anodes along the pile length. Based on ISO recommendation, the prevention current density mainly depends on the oxygen availability for new structures, for which current densities of 0.2 mA·m^{-2} to 2 mA·m^{-2} are commonly applied. In this study, the main part of the design was to calculate the required initial and final currents, which can define the number and sizing of anodes. The required current densities were 1.0 mA·m^{-2} and 0.5 mA·m^{-2} for the initial and final designed current densities, respectively. The sacrificial anodes were then intended to extend the service life of each pile to ten years or more by using the recommendation. The corrosion current from the sacrificial anode was collected using measured voltage drop across resistor calculation. The corresponding corrosion potential has been monitored versus the silver-silver chloride (Ag/AgCl) electrode.

Figure 5. Precast PC 6 m. pile installation and soil survey.

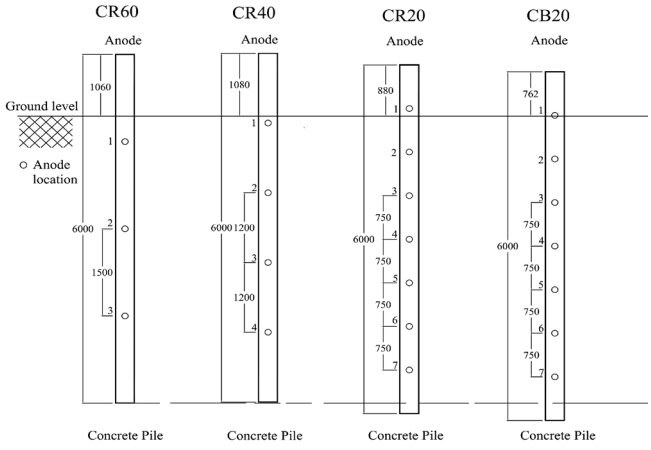

Figure 6. Elevation and anode number location after installation.

Soil resistivity and pH are two of several factors that determine the corrosivity of soil. Soil resistivity is a measure of data to support electrochemical corrosion by migration of charged particles, and soil pH is a measure of soil acidity. Both influence the corrosion of metals underground [19]. However, resistivity and pH are not the only factors affecting corrosion. Total acidity, aeration, moisture content, soil type, soil permeability, soil composition, and heterogeneity are all factors that play a role in determining the corrosivity of a given soil [20,21]. Because of the natural heterogeneity of soil, there is also no single value of resistivity or pH that represents a particular site. The soil pH was measured at this construction site; the result was 7.4. The soil resistivity test results were 400 Ω·cm to 800 Ω·cm. The project area has demonstrated a high corrosion severity of soil based on EN. 12501-2 [22] standard. In addition, salinity is also a factor affecting the deterioration of concrete. The condition at the concrete placement site in an area where it is suspected that a sulfate attack will occur due to an external source of sulfate migrating into the concrete has to be considered. Proportioning guidelines for concretes that will be exposed to sulfate-containing solutions have been established by the ACI standard [23]. Both chloride and sulfate content of soil were collected (Figure 5) and evaluated by titration.

Soil salinity was assessed by drilling four boreholes at each pile specimen to a depth of 6 m. Soil samples were collected at 1m intervals along the 6 m length, and the concentrations of chloride and sulfate ions were determined through titration. Figure 7 illustrate the water-soluble chloride and sulfate contents for soil samples at the construction site. The data revealed an increase in chloride levels with depth until 4 m, followed by a decrease at 6 m. The highest observed chloride content was 0.14% by weight. However, no specific guidelines or threshold limits for chloride concentration in the soil and its influence on reinforcement corrosion have been established and salinity is unequal for all locations and depths [24,25]. The chloride effect is intricate and heavily reliant on numerous factors, such as the composition of cementitious and/or pozzolanic materials used in the concrete [35].

The degree of exposure must be assessed based on the sulfate concentration in the soil. Soil samples indicate exposure levels as negligible, moderate, severe, or very severe, in accordance with the ACI standard [23]. In the salinity soil survey conducted at the construction site, most soil samples exhibited severe sulfate exposure ($0.20 \leq SO_4 \leq 2.0\%$ by weight). Concrete structures exposed to water-soluble sulfates from external sources are prone to significant deterioration. This is a common issue, especially in areas where the soil contains higher sulfate concentrations in contact with concrete. Concrete structures can show signs of sulfate attack through three types of phenomena when exposed to external sulfates: chemical sulfate attack, as well as physical sulfate attack caused by the crystallization of certain sulfate salts. As a result, the chloride and sulfate contents indicate that both of these soil parameters may equally contribute to the assessment of soil corrosivity [26-30].

2.5 Test procedure

2.5.1 Compressive strength test

Prior to conducting the accelerated test and driving the pile to the ground, three-cylinder samples underwent compressive strength testing according to ASTM C39 [31]. The compressive strength of the concrete was determined through a fracture test of the concrete cylinder, which measured 150 mm in diameter and 300 mm in height. Each sample was tested at the ages of 7 day and 28 day. The results from the three samples were averaged to obtain the concrete specimen's overall result. It was ensured that all specimens were handled with utmost care during lifting and transportation to the site, preventing any damage and maintaining the integrity of the results.

2.5.2 Rapid chloride permeability

The Rapid Chloride Permeability Test (RCPT) is a widely used method to evaluate concrete's resistance to chloride ion ingress. This test assesses the electrical conductance of a concrete mix and indicates its ability to resist the penetration of chloride ions. The test involves monitoring the amount of electrical current passing through concrete specimens. The testing procedures are standardized in ASTM Standard [32]. For this test, three concrete samples, each with a thickness of 50 mm and a diameter of 100 mm, were used. The test was conducted when the concrete was 28 days age. During the test, one end of the concrete surface was in contact with sodium hydroxide solution, while the other end was in contact with sodium chloride solution. The resistance of the concrete to the penetration of chloride ions was determined by measuring the total charge passed through the specimens over a period of 6 h. A potential difference of 60VDC was maintained across the specimen. According to ASTM C1202 [32] (Table 2), the results were compared with the suggested limits for chloride ion penetrability. Assessing the resistance of concrete to chloride ion penetration is crucial for protecting reinforced concrete structures from premature deterioration and corrosion.

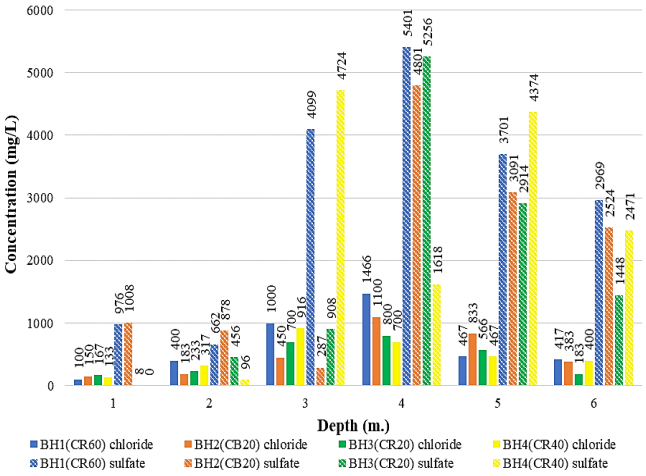

Figure 7. Chloride and sulfate concentration in soil construction site.

Table 2. Recommendation of chloride ion penetrability.

Charge passed (coulombs)	Chloride ion permeability
>4000	High
2000 to 4000	Moderate
1000 to 2000	Low
100 to 1000	Very low
100 to 1000	Negligible

2.5.3 Surface resistivity

The surface resistivity test was carried out on three cylindrical concrete samples, each with a diameter of 150 mm and a height of 300 mm. After the samples were cast and cured, they were submerged in water for one day to test under saturated surface dry condition (SSD) at the ages of 7 day and 28 day. The test utilized the widely recognized Wenner four-probe method, which conforms to the AASHTO T358 [33] standard. In this method, an electrical current is applied between the outer electrodes, while the potential difference is measured between the two inner electrodes to accurately determine the concrete resistivity.

2.5.4 Half-cell potential measurement

The half-cell potential measurements for the accelerated test were measured using a standard copper/copper-sulfate electrode (CSE) [17]. The tests were performed at three points along the length of the PC specimen at 0, 500, and 1000 mm.

3. Results and discussion

3.1 Compressive strength

The compressive strength results were 25 MPa and 35 MPa at 7 day and 28 day, respectively. The strength development pattern is generally consistent with the age of concrete. Generally observed, the high early strength development of the concretes can be attributed to Portland cement Type III. These effects are responsible for the early strength development in cement. The strength of this study gradually increased. It is the effect of curing because all specimens were cured without continuous watering at the casting yard. Concrete curing controls and prevents high evaporation from the concrete setting. Since water is the most important element for hydration control, it certainly affects concrete strength in maintaining the remaining humidity for at least seven days. The concrete strength will be increased as long as sufficient moisture allows cement to react with water. The period in preventing and maintaining moisture inside with a bath is called the curing period [34]. The strength rises rapidly in the first phase and slows down later because of the proper humidity and temperature reasons caused [35]. The correlation can be seen after air and wet curing; the capacity is higher in wet curing day and night. It cannot be accomplished by damp curing for [36] a long time due to the limitations of the construction. Therefore, 7 day to 14 day for continuous wet curing was already appropriate [37].

3.2 Rapid chloride permeability

Three samples were also investigated using the RCPT test. The results of the total charge passed were 7138, 5940, and 6412 coulombs. The average result was 6497 coulombs. The results of chloride ion penetrability based on the charge passed were high, and the results at 28 days indicated a high potential for corrosion. The RCPT and surface resistivity test results in this study correlate reasonably well with Chini's relationship and the proposed Rupnow relationship. Several [38-45] have conducted RCPT tests from various states and found a strong relationship between RCPT and resistivity tests. Chini *et al.* [38] were the first to demonstrate this correlation by procuring concrete test cylinders from ongoing construction projects during their research. They tested 120 samples at 28 days for SR and RCPT from Class IV concrete (compressive strength 37.9 MPa) and proposed the relationship. The average result of Chini's studies revealed that the Class IV concrete samples (Portland cement type III) were 2948 coulombs at 28 days of the test. The maximum value was 8403 coulombs. Rupnow *et al.* [40] tested over 30 laboratory mixtures with various combinations of cementitious and water-cementitious materials ratios (w/cm). They also examined some field samples to establish the relationship between RCPT and resistivity tests.

Under high risk of corrosion, the corrosion may be minimized by the use of corrosion-resistant materials and/or the cathodic protection system. For utilizing corrosion-resistant materials, concretes produced using the pozzolanic materials in cement had lower chloride permeability compared to those of pure Portland cement. The concretes produced using the ordinary portland cement had demonstrated the very high chloride permeability for all blended cement concrete. Moreover, by using more special cements such as granulated blast-furnace slag cements have proved to give a very high resistance of concrete against chloride penetration compared to that of pure portland cements [46]. It is therefore pozzolanic materials have been used for improved durability of concrete structures in severe chloride containing environments [47-50]. Thus, precast prestressed concrete using only pure portland cement may has been a major concern of corrosion risk.

3.3 Surface resistivity

Surface resistivity was measured according to AASHTO T 358 [33]. This test method involves evaluating the electrical resistivity of concrete samples to assess their resistance to chloride ion penetration quickly. The results of concrete surface resistivity of cylindrical concrete samples were 5.84 kΩ·cm and 6.40 kΩ·cm at 7 day and 28 day of age, respectively. The resistivity of concrete increased with time. The result of 28 days was about 9.40% higher than the seven days age. In this case, the resistivity results obtained are slightly lower than anticipated. Concrete curing in the casting yard may affect the resistivity results. The control mixture of Portland cement type III did not show a significant increase beyond seven days as the majority. According to [51], there were slight differences between their results and this study. In their research, 75 concrete mixtures were made in the laboratory. The concrete mixtures varied in water-to-cementitious materials (w/cm) (0.40, 0.45, and 0.50 w/cm). Then, the resistivity was established and concluded. The results revealed a very high probability of chloride ion penetration and indicated the same trend as the RCPT evaluation. The relationships between resistivity and RCPT results were compared, and a reasonably good correlation was found between the results of this study.

High corrosion risk on corrosion, there are alternative corrosion prevention techniques by using corrosion-resistant materials and the cathodic protection system. Due to corrosion concerns, corrosion may occur on this type of cement rather than pozzolanic cement. Pozzolan material increases in electrical resistivity at later ages, consistent with the pozzolanic reaction that occurs at later ages for many alternative pozzolan materials [52-55]. The pozzolanic reaction rate depends on several factors, such as the composition of the pozzolan material,

replacement level, and temperature [52, 54-57]. These factors may result in a variety of corrosion prevention levels.

Nevertheless, cathodic protection is one of the most popular preventative techniques for controlling corrosion. Although used in numerous applications in prestressed concrete structures, many untapped opportunities exist to apply this technology. According to ISO standards, the cathodic protection system could help prevent corrosion.

3.4 Half-cell potential and corrosion current density

Two specimens of each sacrificial anode type were electrically accelerated. The polarization and depolarization of the PC wire were investigated. The potential shift was recorded using a copper/copper sulfate electrode (CSE). Cathodic protection applied to steel in concrete is usually considered adequate if the 100 mV decay criterion is fulfilled. This criterion is also recommended by the ISO standard. Instantaneous OFF potential more negative than 100 mV was measured before the corrosion accelerated test to ensure that all sacrificial anode types delivered an appropriate cathodic polarization current to the specimens. The polarization decay results of two PC specimens embedded with CB20 are demonstrated in Figure 8. The measured distances were 0.5 (0.15 m from anode installation) and 1.0 m (0.65 m from anode installation) from one end. The polarization decay results of all specimens are summarized in Figure 9. The results show that the effective polarization distance from the anode position ranged from 400 mm to 600 mm for each anode type. The results were confirmed by Wanchai Yodsudjai and Salila Rakvanich [58] and Ha *et al.* [59] that the anode life increased with increasing concrete quality and decreased with increasing environmental severity. The effective distance was approximately 400 mm to 600 mm from the anode-installed position. The effective distance was determined by distance influenced by the polarization effect of the sacrificial anode in concrete slabs and beams.

In order to study the short-term corrosion characteristics of PC and non-PC samples, the positive terminal of the rectifier was linked to the steel wire, while the negative terminal was attached to the zinc plate. The accelerated test was energized using a rectifier. The measured current density results were plotted to compare each sacrificial anode type's corrosion behavior and durability, as presented in Figure 10. The control specimen results considerably stayed constant until cracking occurred. In addition, for CB20, CR20, and CR40 specimens, the current density results demonstrated differences from CT before failure occurred about 50 h. The current density results before failure were rapidly increased. The discharged current densities should be from both PC wires and sacrificial anodes. For the CR60 specimen, the results were more stable than the others, which may be due to the biggest zinc use in this anode type. However, in high current density from the rectifier, the sacrificial anode could extend 29.4% to 51.5% of the accelerated corrosion time (Figure 11). The cumulative electric charges passed in CT, CB20, CR20, CR40, and CR60 were 2116302, 3171403, 3150439, 2664146, and 2729615 coulombs. These results were correlated with the accelerated corrosion time, which showed that the sacrificial anode could prolong the lifetime between 25.9% to 49.9% of CT specimens. Theoretically, the performance of CR60 and CR40 in this test should be better than that of CR20 and CB20. However, due to corrosion products, multiple cracks occurred in each concrete sample along the length. All four main steel were corroded at the same time. In this test, the failure condition of the concrete specimen was defined as a crack that had to be more than 100 mm in length. Determining the crack length was straight forward by using simple measuring tapes. Cracks were induced in cover concrete because the volume of the corrosion product was much larger than that of the original steel. Variation in crack growth could be expected to occur on the test. The width of surface cracks depends on the formation of corrosion products and the resulting crack pattern [60]. The variation caused changes in cracking time at the failure of CR60.

For non-PC specimens, the PC wire was not in prestressed condition. This experimental study focused on the different corrosion behavior between prestressed and non-prestressed wire under severe conditions. All specimens' results were in the same trend. The current density was gradually reduced throughout the accelerated time. Due to the concrete covering of non-PC specimens being more than that of PC specimens, the accelerated time before failure can be extended with higher current density. The current density results showed that CR60 (PC7 and PC8) rapidly increased with the highest peak among the others. The CB20 (PC14 and PC15) was also observed to be at the peak. This peak was not observed in PC specimens. The specimens containing a sacrificial anode significantly aided in polarizing the steel wire, as illustrated in Figure 12.The sacrificial anode could extend 6.4% to 12.7% of the accelerated corrosion time than the CT (PC23 and PC24) presented in Figure 13. The cumulative electric charge passed in CT, CB20 and CR60 were 18622211, 23326003 and 29520313coulombs. These results were in the same trend with the accelerated corrosion time that the sacrificial anode could extend the life time between 25.2% to 58.5% of CT specimens.

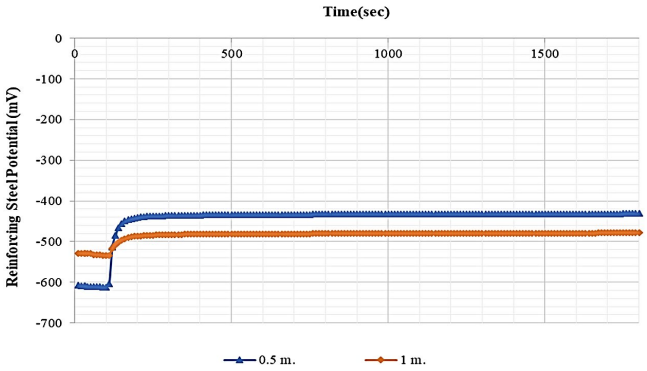

Figure 8. Polarization decay results of sacrificial anode CB20 for PC specimen.

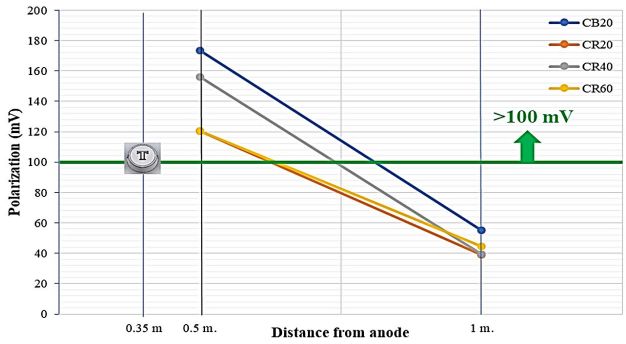

Figure 9. Polarization decay results of all sacrificial anode types for PC specimen at different distance.

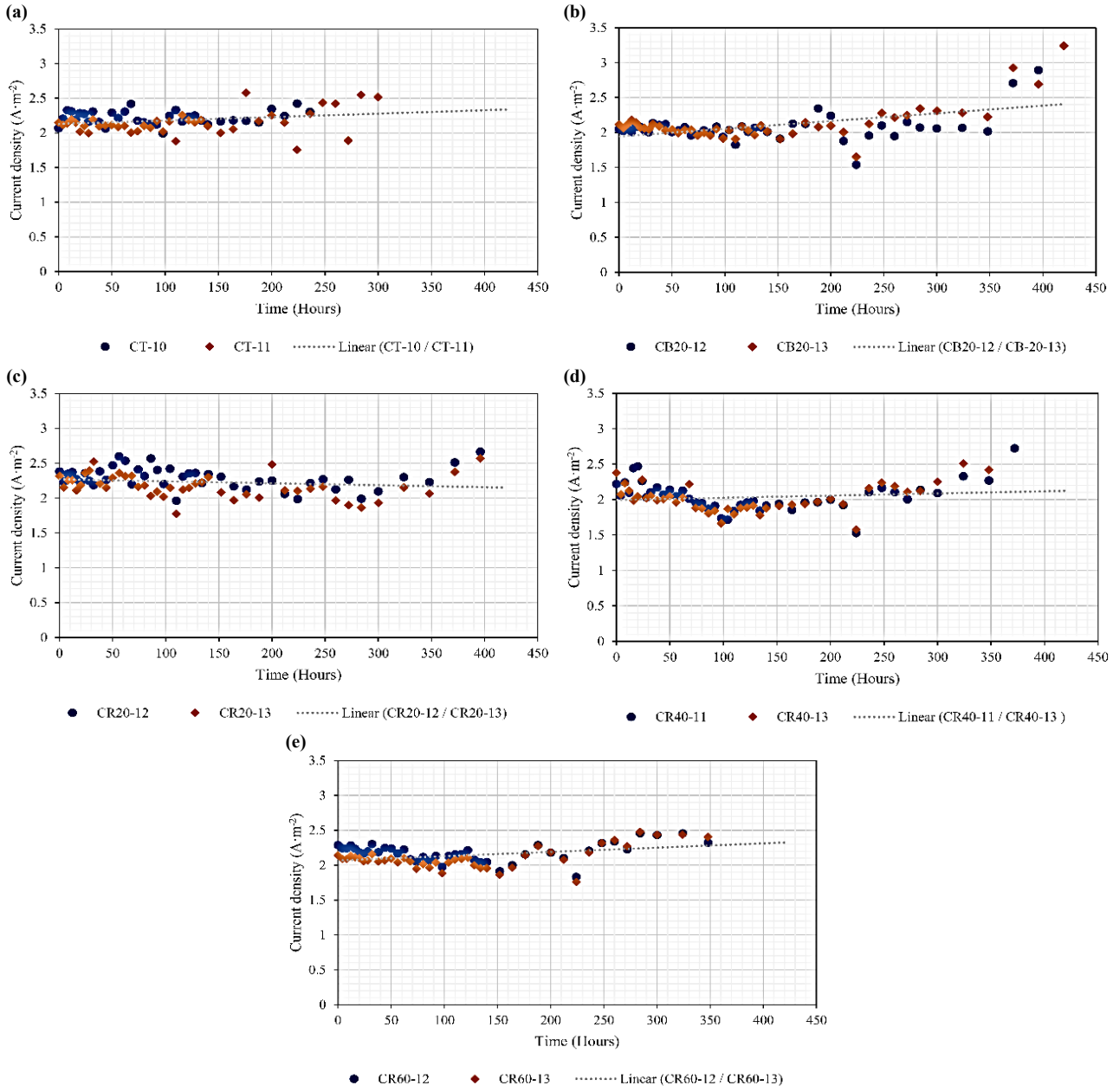

Figure 10. Current density results for PC specimen (a) CT, (b) CB20, (c) CR20, (d) CR40. and (e) CR60.

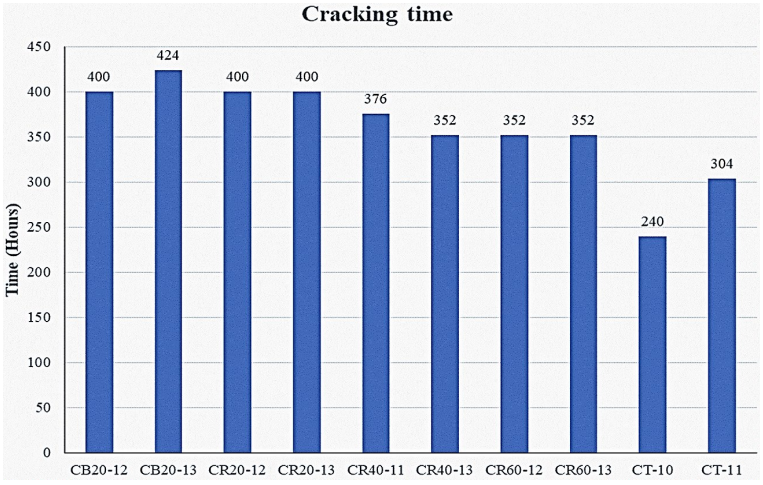

Figure 11. Total corrosion accelerated time before concrete cracking for PC specimen.

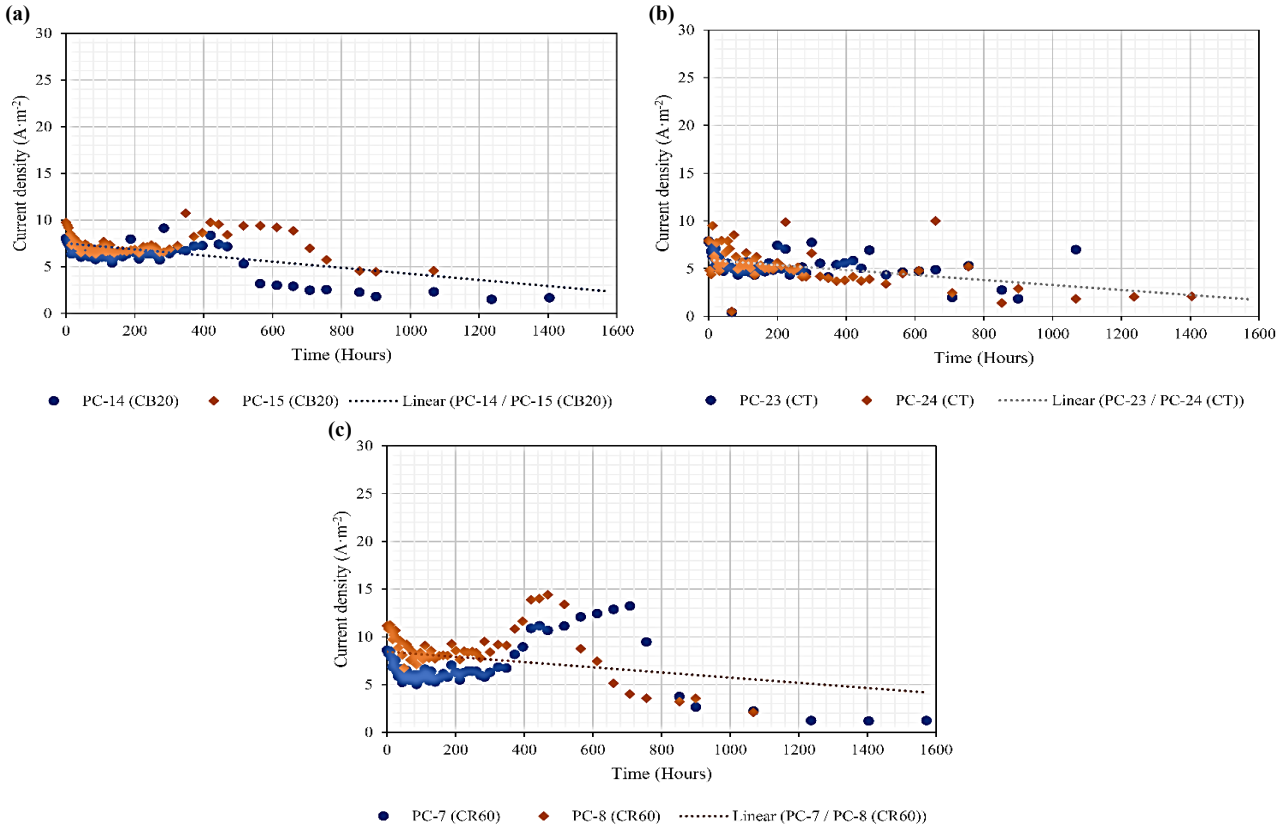

Figure 12. Current density of non-PC specimen; (a) CT, (b) CB20. and (c) CR60.

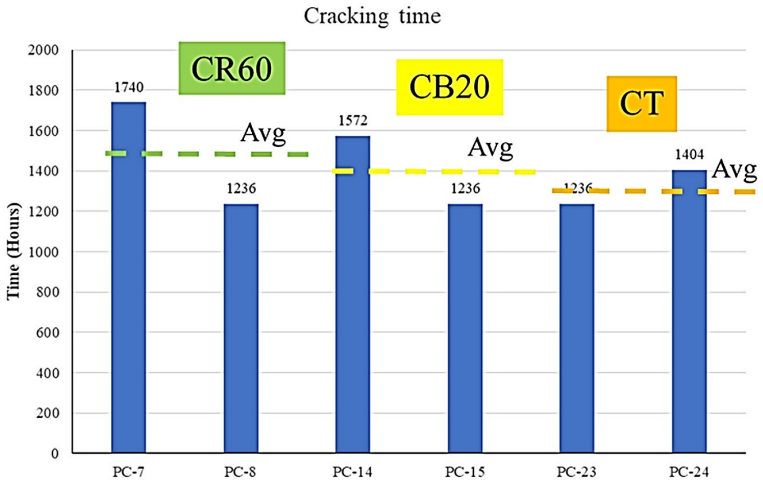

Figure 13. Total corrosion accelerated time before concrete cracking for non-PC specimen.

The objective is to investigate the long-term corrosion resistance of precast prestressed concrete (PC) members when subjected to severe environmental conditions, leveraging the implementation of a galvanic cathodic protection system. The current density distributions along the steel wire delivered by sacrificial anode polarization continuing over the entire length of large PC specimens were monitored and presented in Figure 14. After specimen installation, the current density for all sacrificial anode types along the steel wire was 7 $mA{\cdot}m^{-2}$ to 13 $mA{\cdot}m^{-2}$, significantly higher than 2 $mA{\cdot}m^{-2}$, and was then mainly constant to 0.3 $mA{\cdot}m^{-2}$ to1 $mA{\cdot}m^{-2}$. The protection efficiency was improved when the sacrificial anode was embedded in the specimen. Compared with CB20 and CR20, the corrosion current density results of CB20 were higher than those of CB20 at first and then decreased faster than those of CR20 due to the anode shape effect. CB20 had a surface area of more zinc than CR20, about 24%. The CB20 and CR20 became more stable around 100 day to 200 day after specimen installation. In addition, for the bigger sizes of the anode (CR40 and CR60), the corrosion current density results were gradually decreased, followed by a stable corrosion current density (between 0 $mA{\cdot}m^{-2}$ to 0.5 $mA{\cdot}m^{-2}$).

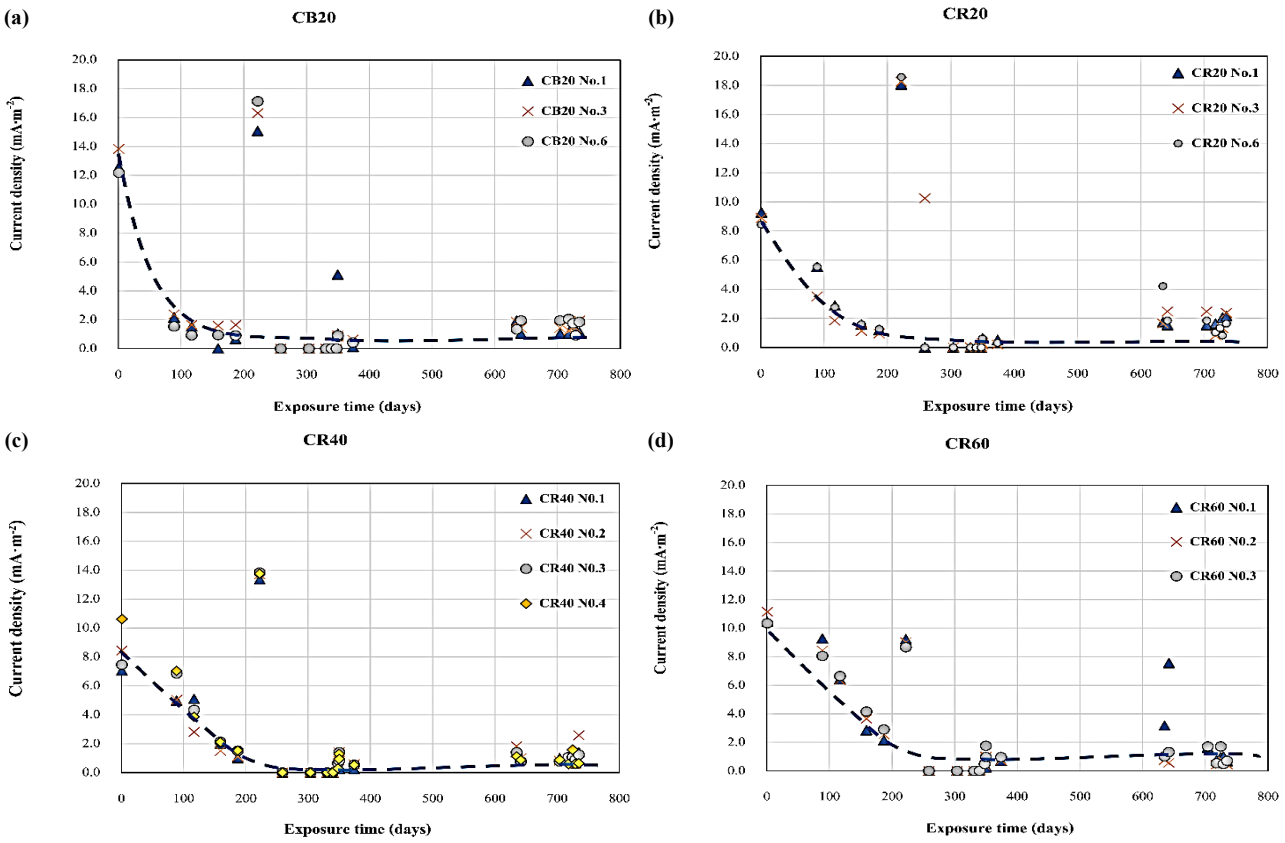

Figure 14. Corrosion current density of PC wire in large PC specimen along the length; (a) CB20, (b) CR20, (c) CR40, and (d) CR60.

The stable corrosion current density was around 250 days after installation. CR40 and CR60 are positioned at a greater distance from the anode, which may account for this. Both specimens showed a uniform distributed current in protection. The design calculation specified both the initial and final design current densities. It also determined the expected cathodic current density demand necessary to achieve efficient cathodic protection of concrete structures within a relatively short period. The initial design cathodic current density was necessarily higher than the final design current density because the calcareous scale developed during the initial phase reduces the subsequent current demand as the polarization resistance is reduced. Calculating the necessary number of specific anodes to achieve sufficient polarizing capacity relies on determining the initial and final current densities. A service life prediction for sacrificial anode was based on the measured current in the field. The theoretical calculation for zinc's mass loss was done using Faraday's law. The calculation of service life used the acquired data of the current from 350 day to 735 day. The remaining service life of the anodes was calculated by assuming a constant consumption. The estimated service life of the anode is 7 year to 8 year. These values are the same trend as Sergi's research [61]. The results showed a good agreement with the design's current density. In actual conditions for concrete structures using zinc anode, Ha *et al.* [62] stated that sustainable protection exists under low resistivity if the steel is surrounded by seawater or underground. Some degree of partial protection was noted, attributed to the ability to modify depolarization levels based on the specific resistivity of the concrete, which is influenced by factors such as precipitation, humidity, and ambient weather conditions.

4. Conclusions

The investigation aims to analyze the potential corrosion of a prestressed concrete structure by subjecting it to different types of sacrificial anodes. The study investigates the effectiveness of each anode variant in preventing corrosion and provides valuable insights into the long-term durability of the structure.

1. In the initial short-term test, before the accelerated test, all types of sacrificial anodes demonstrated promising performance on precast prestressed concrete piles. This performance was in accordance with the ISO standard 100 mV, indicating their potential effectiveness in preventing corrosion. The following conclusions are drawn:
2. The effective distance was approximately 400 mm to 600 mm from the anode-installed position.
3. Sacrificial anode showed good agreement results to resist corrosion of PC and non-PC cylinder specimens.
4. The macrocell data from the large PC specimens indicated that all sacrificial anodes met the cathodic prevention criteria outlined in the ISO standard, maintaining a protective current of 0.2 $mA{\cdot}m^{-2}$ to 2 $mA{\cdot}m^{-2}$. It's worth noting that the corrosion current for CB20 and CR20 stabilized after 100 days, while for C40 and CR60, it took around 250 days to stabilize. This demonstrates compliance with the ISO standard, attributed to the different spacing of each sacrificial anode type.
5. The study's findings have real-world relevance, particularly in practical, real-world conditions. Extensive exposure to saline soil revealed the highly effective application of driven precast prestressed concrete piles with installed sacrificial anodes in preventing corrosion

within the construction industry. The estimated service life of 7 year to 8 year, aligned with the designed current density, further underscores the potential for innovative product development of an integrated corrosion protection system for the construction sector.

Acknowledgment

The authors gratefully acknowledge the support provided by the Faculty of Engineering at Kamphaeng Saen, Kasetsart University.

References

[1] P. Ghods, O. B. Isgor, and M. Pour-Ghaz, "A practical method for calculating the corrosion rate of uniformly depassivated reinforcing bars in concrete," *Materials and Corrosion,* vol. 58, no. 4, pp. 265-272 2007.

[2] G. Koch, J. Varney, N. Thompson, O. Moghissi, M. Gould, and J. Payer, *International Measures of Prevention, Application, and Economics of Corrosion Technologies Study*, NACE Impact Report, 216 pages, 2016.

[3] R. B. Polder, W. H. A. Peelen, B. T. J. Stoop, and E. A. C. Neeft, "Early stage beneficial effects of cathodic protection in concrete structures", *Materials and Corrosion*, vol. 62, no. 2, pp. 105-110, 2011.

[4] J. Xu, and W. Yao, "Current distribution in reinforced concrete cathodic protection system with conductive mortar overlay anode," *Construction and Building Materials*, vol. 23, no.6, pp. 2220-2226, 2009.

[5] A. Byrne, N. Holmes, and B. Norton, "State-of-the-art review of cathodic protection for reinforced concrete structures", *Magazine Concrete Research*," vol. 68, pp. 1-14, 2016.

[6] P. Pedeferri, "Cathodic protection and cathodic prevention," *Construction and Building Materials*, vol. 10, pp. 391-402, 1996.

[7] L. Bertolini, F. Bolzoni, M. Gastaldi, T. Pastore, P. Pedeferri, and E. Redaelli, "Effects of cathodic prevention on the chloride threshold for steel corrosion in concrete," *Electrochimica. Acta*, vol. 54, pp. 1452-1463, 2009.

[8] J. Bennett, J. B. Bushman, J. Costa, and P. Noyce, "Field application of performance enhancing chemicals to metallized zinc anodes," *Corrosion*, No. NACE-00790, 2000.

[9] J. Xu, and W. Yao, 'Current distribution in reinforced concrete cathodic protection system with conductive mortar overlay anode," *Construction and Building Materials*, vol. 23, pp. 2220-2226, 2009.

[10] P. Marcassoli, A. Bonetti, L. Lazzari, and M. Ormellese, "Modeling of potential distribution of subsea pipeline under cathodic protection by finite element method," *Materials and Corrosion*, vol. 66, pp. 619-626, 2015.

[11] N. Khomwan, and P. Mungsantisuk, "Startup Thailand: A new innovation sacrificial anode for reinforced concrete structures," *Engineering Journal*, vol. 23, no. 4, pp. 235-261, 2019.

[12] Highways England, CS 462, *Repair and management of deteriorated concrete highway structures*, 2020.

[13] N. Krishnan, D. K. Kamde, Z. D. Veedu, R. G. Pillai, D. Shah, and V. Rajendran, "Long-term performance and life-cycle-cost benefits of cathodic protection of concrete structures using galvanic anodes", *Journal of Building Engineering*, vol. 42, p. 102467, 2021.

[14] D. K. Kamde, K. Manickam, R. G. Pillai, and G. Sergi, "Long-term performance of galvanic anodes for the protection of steel reinforced concrete structures", *Journal of Building Engineering*, vol. 42, p. 103049, 2021.

[15] EN ISO 12696 Standards, "Cathodic Protection of Steel in Concrete," 54 pages, 2022.

[16] Build NT 356, "Concrete, repairing materials and protective coating: embedded steel method, chloride permeability," NT Build, 356, Nordtest, Espoo, Finland, 1989.

[17] ASTM C876-22b, "Standard test method for corrosion potentials of uncoated reinforcing steel in concrete, Annual Book of ASTM Standards," 8 pages, 2022.

[18] ASTM G1, "Standard practice for preparing, cleaning, and evaluating corrosion test specimens, Annual Book of ASTM Standards," 9 pages, 2017.

[19] M. Romanoff, *Underground Corrosion*, National Bureau of Standards Circular 579, April 1957.

[20] N. D. Tomashov, and Y. N. Mikhailovsky, "Corrosivity of Soil," *Corrosion*, vol. 15, no. 2, pp. 41-46, 1959.

[21] National Bureau of Standards, "Study of causes and effects of underground corrosion," *Journal AWWA*, Dec., pp. 1581-1588, 1958.

[22] BS EN 12501-12502, "Protection of metallic materials against corrosion. Corrosion likelihood in soil, Part 2: Low alloyed and unalloyed ferrous materials" European Standard, 2003.

[23] American Concrete Institute, *ACI manual of concrete practice. Part 3*. Farmington Hills, MI. 2004.

[24] M. Maslehuddin, M. M. Al-Zahrani, M. Ibrahim, M. H. Al-Mehthel, and S. H. Al-Idi, "Effect of chloride concentration in soil on reinforcement corrosion," *Construction and Building Materials*, vol. 21, no. 8, pp. 1825-1832, 2007.

[25] S. K. Al-Mamoori, L. A. J. Al-Maliki, K. El-Tawel, H. M. Hussain, "Chloride, calcium carbonate and total soluble salts contents distribution for An-Najaf and Al-Kufa Cities' soil by using GIS," *Geotechnical and Geological Engineering*, vol. 37, no. 3, pp. 2207-2225, 2019.

[26] S. H. Kosmatka, and M. L. Wilson, *Design and Control of Concrete Mixtures*. Fifteenth Edition, Engineering Bulletin 001.15, Portland Cement Association, Skokie, IL, 444 pages, 2011.

[27] P. K. Mehta, *Concrete: Structure, Properties and Materials*. Prentice Hall, Englewood Cliffs, NJ. 1986

[28] D. Stark, *Performance of Concrete in sulfate Environments*, PCA RD129, Portland Cement Association, Skokie, IL, 28 pages, 2002.

[29] H. Haynes, R. O'Neill, M. Neff, and P. K. Mehta, "Concrete deterioration from physical attack by salts," *Concrete International*, vol. 18, no. 1, pp. 63-68., 1996

[30] H. Haynes, and M. T. Bassouni, "Physical salt attack on concrete," *Concrete International*, vol. 33, no. 11, pp. 38-42, 2011.

[31] ASTM C39/39M-21, "Standard test method for compressive strength of cylindrical concrete specimens, Annual Book of ASTM Standards," 8 pages, 2021.

[32] ASTM C1202-19, "Standard test method for electrical indication of concrete's ability to resist chloride ion penetration, Annual Book of ASTM Standards," 8 pages, 2019.

[33] AASHTO T358, "Standard method of test for surface resistivity indication of concrete's ability to resist chloride ion penetration," American Association of State Highway and Transportation Officials, Washington, DC, 2015.

[34] R. H. Faraj, A. F. H. Sherwani, and A Daraei. "Mechanical, fracture and durability properties of self-compacting high strength concrete containing recycled polypropylene plastic particles," *Journal of Building Engineering*, vol. 25, 2019.

[35] S. Bahij, S. Omary, F. Feugeas, and A. Faqiri, "Fresh and hardened properties of concrete containing different forms of plastic waste –A review," *Waste Manage*, vol. 113, pp. 157-175, 2020.

[36] P. O. Awoyeraa, and A. Adesinab, "Plastic wastes to construction products: Status, limitations and future perspective," *Case Studies in Construction Materials*, vol. 12, 2020.

[37] G. Madhu, H. Bhunia, P. K. Bajpai, and V. Chaudhary, "Mechanical and morphological properties of high density polyethylene and poly-lactase blends," *Journal of Polymer Engineering*, vol. 34, no. 9, pp. 813-821, 2014.

[38] A. Chini, L. Muszynski, and J. Hicks, "Determination of acceptance permeability characteristics for performance-related specifications for portland cement concrete," *Publication BC 354-41*, University of Florida, Gainesville, FL, 162 pp., 2003.

[39] R. Kessler, R. Powers, E. Vivas, M. Paredes, and Y. Virmani, "Surface resistivity as an indicator of concrete chloride penetration resistance," *Concrete Bridge Conference*, St. Louis, MO, May 4-7, 2008.

[40] T. Rupnow, and P. J. Icenogle, *Evaluation of Surface Resistivity Measurements as an Alternative to the Rapid Chloride Permeability Test for Quality Assurance and Acceptance*, Louisiana Transportation Research Center, Project Report, Baton Rouge, LA, July, 68 pp., 2011.

[41] E. W. Ryan,, *Comparison of Two Methods for the Assessment of Chloride Ion Penetration in Concrete: A Field Study*, master's thesis, University of Tennessee, Knoxville, TN, pp. 42-43., 2011.

[42] R. Spragg, Y. Bu, K. Snyder, D. Bentz, and J. Weiss, "Electrical Testing of Cement-Based Materials: Role of Testing Techniques, Sample Conditioning, and Accelerated Curing," *Publication FHWA/IN/JTRP-2013/28*, Joint Transportation Research Program, Indian Department of Transportation and Purdue University, West Lafayette, IN, pp. 1-16., 2013.

[43] R. Spragg, J. Castro, T. Nantung, M. Parades, and W. Weiss, "Variability analysis of the bulk resistivity measured using concrete cylinders," SPR-3509, FHWA/IN/JTRP-2011, *Joint Transportation Research Program, Washington*, DC, pp. 1-8., 2011.

[44] R. Spragg, C. Villani, K. Snyder, D. Bentz, J. Bullard, and J. Weiss, "Electrical resistivity measurements in cementitious systems: Observations of factors that influence the measurements," *Transportation Research Board*, Washington, DC, pp. 90-98, 2013.

[45] J. Tanesi, and A. Ardani, "Surface resistivity test evaluation as an indicator for the chloride permeability of concrete," *FHWA Publication* No: FHWA-HRT-13-024, Turner-Fairbank Highway Research Center, McLean, VA, 2013.

[46] P. K. Mehta, and P. J. M. Monterio, *Concrete*. New York: McGraw-Hill; 2006.

[47] J. Bijen, *Blast furnace slag cement for durable marine structures*. The Netherlands: VNC/BetonPrisma., 1998.

[48] J. Hill, and J. H. Sharp, "The mineralogy and microstructure of three composite cements with high replacement levels," *Cement and Concrete Composites,* vol. 24, no. 19, pp. 1-9, 2002.

[49] S. Hu, X. Guan, and Q. Din, "Research on optimizing components of microfine highperformance composite cementitious materials," *Cement and Concrete Composites,* vol. 32, no. 12, pp. 1871-1875, 2002.

[50] O. Sengul, and O. E. Gjørv, "Effect of binder system on the resistance of concrete against chloride penetration" *8th international symposium on utilization of high-strength and high-performance concrete*, Tokyo, pp. 330-335, 2008.

[51] J. A. Hartell, and C. Shults, *Surface Resistivity Testing for Quality Control of Concrete Mixtures*, Southern Plains Transportation Center United States. Department of Transportation. University Transportation Centers (UTC) Program, Report No. SPTC 17.1-07, pp. 50, 2018.

[52] ACI Committee 201, "Guide to Durable Concrete, American Concrete Institute," 2016.

[53] A. Scott, and M. Alexander, "Effect of supplementary cementitious materials (binder type) on the pore solution chemistry and the corrosion of steel in alkaline environments," *Cement and Concrete Research*, vol. 89, pp. 45-55, 2016.

[54] C. C. Ferraro, J. M. Paris, T. Townsend, and M. Tia, *Evaluation of Alternative Pozzolanic Materials for Partial Replacement of Portland Cement in Concrete*", FDOT Final Report, 345 pages, 2016.

[55] B. Lothenbach, K. Scrivener, and R. Hooton, "Supplementary cementitious materials," *Cement and Concrete Research*, vol. 41, no. 12, pp. 1244-1256, 2011.

[56] H. F. Taylor, *Cement Chemistry*, second ed., Thomas Telford, 1997.

[57] J. M. Paris, J. G. Roessler, C. C. Ferraro, H. D. DeFord, and T. G. Townsend, "A review of waste products utilized as supplements to Portland cement in concrete", *Journal of Cleaner Prodroduction*, vol. 121, pp. 1-18, 2016.

[58] W. Yodsudjai, and S. Rakvanich, "Experimental study on anode life and effective distance of sacrificial cathodic protection in reinforced concrete," *Engineering Journal*, vol. 24 no. 6, pp. 159-169, 2020.

[59] J.-M. Ha, J.-A. Jeong, and C. Jin, "Development of conductive mortar for efficient sacrificial anode cathodic protection of reinforced concrete structures—Part 1: Laboratory experiments," *Applied Science*, vol. 12, no. 23, pp. 1-14, 2022.

[60] A. E. A. Thybo, *Corrosion-induced Cracking in Reinforced Concrete Structures -a numerical study.* Technical University of Denmark, Department of Civil Engineering. B Y G D T U. Rapport No. 397, 2018.

[61] G. Sergi, "Ten-year results of galvanic sacrificial anodes in steel reinforced concrete," *Materials and Corrosion*, vol. 62, no. 2, pp. 98-104, 2011

[62] J.-M. Ha, J.-A. Jeong, and C. Jin, "Development of conductive mortar for efficient sacrificial anode cathodic protection of reinforced concrete structures—Part 2: Four-year performance evaluation in bridges," *Applied Science*, vol. 14, no. 5, pp.1-16, 2024.